Oscillatory amplification of stochastic resonance in excitable systems

E. I. Volkov,[1] E. Ullner,[2] A. A. Zaikin,[2] and J. Kurths[2]

[1]*Department of Theoretical Physics, Lebedev Physical Institute, Leninskii 53, Russia*

[2]*Institut für Physik, Potsdam Universität, Am Neuen Palais 10, D-14469 Potsdam, Germany*

(Received 12 December 2002; published 22 August 2003)

We study systems which combine both oscillatory and excitable properties, and hence intrinsically possess two internal frequencies, responsible for standard spiking and for small amplitude oscillatory limit cycles (Canard orbits). We show that in such a system the effect of stochastic resonance can be amplified by application of an additional high-frequency signal, which is in resonance with the oscillatory frequency. It is important that for this amplification one needs much lower noise intensities as for conventional stochastic resonance in excitable systems.

DOI: 10.1103/PhysRevE.68.026214 PACS number(s): 05.45.−a, 05.40.Ca

I. INTRODUCTION

The response of an excitable system to an external signal is a key effect of information processing in a single excitable oscillator or networks of excitable elements. Several intriguing phenomena have been found in the study of this effect. One of the most interesting and counterintuitive effect is stochastic resonance (SR) [1], initially found in bistable systems [2], and later confirmed in a large variety of physical [1] or biological systems [3], including also noise-induced structures [4] and excitable systems [5]. In SR an optimal amount of noise, acting upon an excitable system, increases the quality of the signal received via noise-induced synchronization [6]. Noteworthy, SR has been also found not only in excitable neural systems itself [7] or brain processing area [8], but also in the behavior of the whole organisms [9]. In spatially extended systems SR manifests itself in the signal transmission, resulted in a noise-induced propagation in bistable [10], excitable [11], or monostable systems [12,13].

In SR a part of the noise energy is used for constructive purposes, to cause a form of synchronization between input and output signals. Several investigations have been performed to find possibilities for the amplification of this effect. Array-enhanced SR has been considered in Refs. [14,15], where it has been shown that embedding of the processing element in a network of elements with optimal coupling and noisy strength [16] can improve the signal. This effect is closely connected and sometimes conceptually indistinguishable from spatiotemporal SR [17] or SR in extended bistable systems [18]. Another possibility to amplify the SR effect has been exploited in Ref. [15] by application of noninvasive control of SR. In this case, the external feedback has enhanced the response of a noisy system to a monochromatic signal. Finally, there were investigations, which have shown that with internal colored noise the SR effect can be enhanced in systems with a large memory time [19].

In this paper we study the SR effect in another class of systems, which differs to already explored ones by the fact that this class possesses properties of both oscillatory and excitable behavior. As a paradigmatic model for such systems we consider the famous FitzHugh-Nagumo (FHN) oscillator, known for its simplicity and rather realistic simulation of neural activity.

Generally, the FHN model is tuned to exhibit either an oscillatory behavior with strongly nonlinear oscillations in the system or an excitable behavior with a stable fix point, and the feature that relatively small perturbations can lead to a large excursion (excursion loop or spike) [20,5,21]. In contrast to this we are interested in a FHN model that is tuned to have both oscillatory and excitatory properties. Such dynamics takes place in FHN-like models [22] or in biophysical models [23,24], if their parameters are chosen in the region of the so-called "Canard" bifurcation [25,26]. In these works a Canard solution is a solution of a singular perturbed system which passes close to a bifurcation point and follows a repelling slow manifold for a considerable amount of time.

For the FHN model the Canard phenomenon means that there are quasiharmonic oscillations with small amplitude and small periods (see Fig. 1). The parameter region between pure excitable and oscillatory cases is typically very narrow if the stiffness of the oscillator is large ($\varepsilon \ll 1$). But the value of stiffness is not obligatory large and is defined by the kinetic parameters of the specific models. A crucial feature of Canard-like behavior is that a very small change in the control parameter may lead to a large difference in the trajecto-

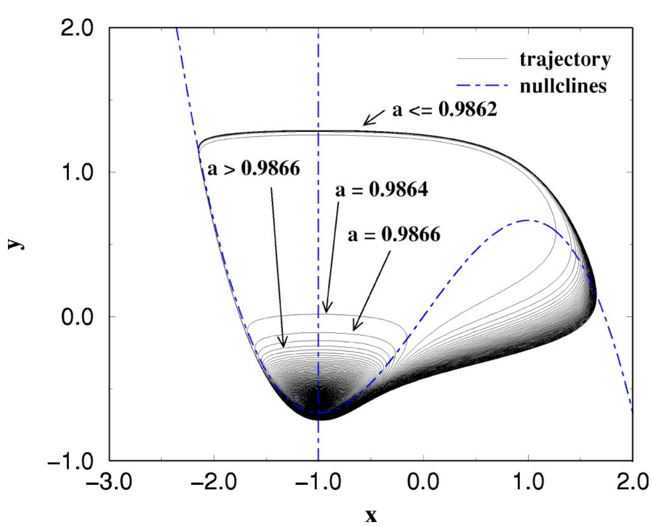

FIG. 1. The dependence of the trajectories and the appearance of Canard trajectories on the parameter *a* in the FHN model without noise and without driving forces.

ries and hence produce oscillations with different frequencies. This change can be also induced by the action of noise, if the system possesses Canard-like oscillations.

The idea to use a system with several intrinsic frequencies as a signal receiver in the presence of noise has been already reported in the literature. For example, in a bistable underdamped system, stochastic resonance may happen both due to intrawell as well as interwell motion [27]. Further on, it was described that nonadiabatic resonance under the action of a high frequency can exist in a noisy excitable system [28]. In all these works, the improvement of a signal processing occurs due to the resonance interplay between an incoming periodic signal and one of the internal frequencies of the oscillating system. In contrast to this case, we consider here the situation in which an additional high-frequency signal improves the detection of a low-frequency signal; i.e., it is crucial that the system is under the action of multifrequency signal. A similar problem formulation was studied in Ref. [29], where it was shown that adding a high-frequency signal may help the detection of a low-frequency signal and leads to a heterodyning effect in a two-dimensional oscillator with one internal frequency near a saddle-node bifurcation. However, this effect occurs due to the action of a resonant high-frequency signal on a detection threshold near a saddle-node bifurcation (see also a case of coupled oscillators [30]), whereas in our case we investigate a noisy system with two different internal frequencies under the action of a two-frequency signal, and the resonance effect at one higher internal frequency leads to the amplification of stochastic resonance at another low frequency.

We consider FHN system under the action of a subthreshold bichromatic signal, which consists of two parts: the first one has the frequency of an investigated signal, and the second one has a higher frequency. We demonstrate the effect of SR amplification, when the higher frequency is in resonance with the frequency of the Canard oscillations of our system. Noteworthy, two-frequency signals are widely used in communications [31], neuroscience [32], laser physics [33], or acoustics [34]. Additionally, the beneficial role of high-frequency (HF) driving has been already found in several biological phenomena, such as increased drug uptake by brain cells [35], improvement of bone and muscle healing [36], or enhanced biodegradation of microorganisms [37]. The effect, presented in this paper, is also closely connected to vibrational resonance (VR) in excitable systems [38], where the high-frequency driving acts as noise and improves the signal processing. VR demonstrates a resonancelike behavior with respect to the amplitude of the HF signal. In contrast to VR, in Canard-enhanced SR it is crucial that not the amplitude but *the frequency* of the HF signal should be in resonance with the oscillatory behavior of a system.

II. THE MODEL

We study the following FHN model:

$$\varepsilon\dot{x}(t)=x(t)-\frac{x(t)^3}{3}-y(t), \tag{1}$$

$$\dot{y}(t)=x(t)+a+\xi(t)+F_{ext}(t), \tag{2}$$

where $\xi(t)$ is Gaussian white noise of the intensity $\langle\xi(t)\xi(t')\rangle=\sigma_a^2\delta(t-t')$ and the parameter a determines the behavior of the system. For $a>1.0$ the FHN model is excitable, and for $a<1.0$ it shows an oscillatory behavior. At the bifurcation point $a=1.0$ the stability of the only fix point $x_f=-a$, $y_f=(a^3/3)-a$ will be changed. Between these two cases an intermediate behavior can appear. For values of the parameter a slightly beyond the bifurcation point, small oscillations near the unstable fix point are existing instead of large spikes. To illustrate this, in Fig. 1 trajectories in the phase space of the FHN system without driving force and noise are plotted in dependence on the parameter a. For $a\leqslant 0.9862$ and $\varepsilon=0.1$, the FHN model oscillates on the well-known big excursion loop. In the intermediate parameter region $0.9864\leqslant a<1$ and $\varepsilon=0.1$, there is also an oscillatory behavior but the loops (Canard-trajectories) in the phase space are much smaller than the excursion loops. Between both possible traces is a clear gap, so that both of these kinds of oscillations can be easily distinguished.

The Canard trajectories exist also for smaller ε-like 0.01, but the intermediate parameter region of a (where Canard oscillations exist) tends to zero for decreasing ε, and the period of subthreshold oscillations near the bifurcation point is $T_{sth}\approx 2\pi\sqrt{\varepsilon}$ [22]. Hence, for $\varepsilon=0.01$ the subthreshold oscillations are very fast, and so the trajectory loops are very small. In the following, we fix the parameter $\varepsilon=0.1$ to have a system with a significant intermediate region where Canard oscillations exist. Similar values of ε (parameter to separate a slow and a fast moving variable) were used also in different papers for the modeling of natural processes [39–41], and so our choice has natural links. In spite of the fact that frequently used harmonic and singular approximations of FHN studies are very suitable for the mathematical tractability of the model behavior, in the real processes the stiffness is in between these two limit cases.

An important fact of the treatment of the Canard oscillations is that a very small change in the parameter a leads to a large difference in the trajectories. This change in the parameter a can be caused by some instantaneous influence of noise. Beside the expected case for the parameter a typical for the Canard phenomenon, Canard-like trajectories can be observed also in the excitable regime $a>1$ close to the bifurcation point if the FHN system is forced by additive noise $\xi(t)$. This can be easily seen in Fig. 2, where trajectories in the phase space were plotted for the parameters $\varepsilon=0.1$, $a=1.01$, $\sigma_a^2=0.0004$ (in the excitable regime), and there is no periodic driving forces. Only the noise drives the FHN system and leads to the Canard-like trajectories and the spikes, and therefore, again the FHN system behaves with two different frequencies of the two cycles, which can be certainly used in signal processing.

These different trajectories manifest themselves in a polymodal interspike interval histogram (ISIH) not only when the parameter a is chosen from the interval corresponding to the Canard orbits (as in Ref. [22]) but for a which provides an excitable regime (see Fig. 3). We have chosen the most pro-

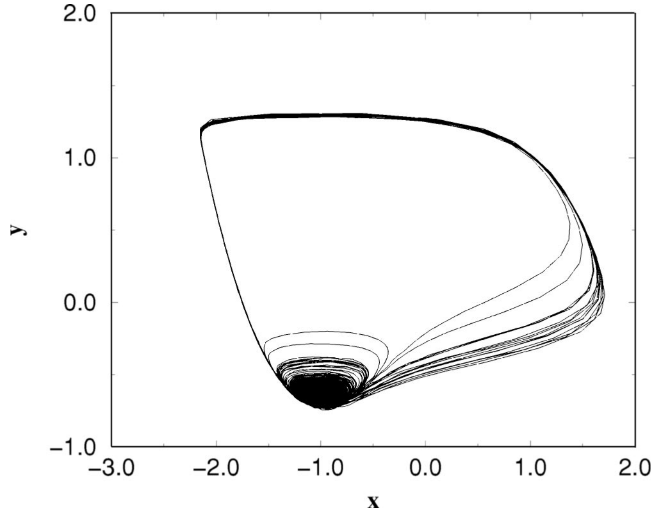

FIG. 2. Occurrence of spike and Canard trajectories in a noise driven FHN model in the excitable regime.

nounced examples of ISIH polymodality but this type of distribution is preserved in some intervals of the essential parameters: $a \in [1.0-1.05], \varepsilon \in [0.2-0.02]$ under the appropriate noise amplitudes.

Next we add a driving force $F_{ext}(t) = b\cos(\omega t)$ and investigate the response of the periodic driven system at the input frequency. To evaluate the amplitude of the input frequency in the output signal, we calculate the Fourier coefficient Q for the input frequency ω. We use the Q parameter instead of the power spectrum because we are interested in the transport of the information encoded in the frequency ω. For this task the Q parameter is a much more compact tool than the power spectrum [1,12]:

$$Q_{\sin} = \frac{\omega}{2n\pi}\int_0^{2\pi n/\omega} 2x(t)\sin(\omega t)\,dt,$$

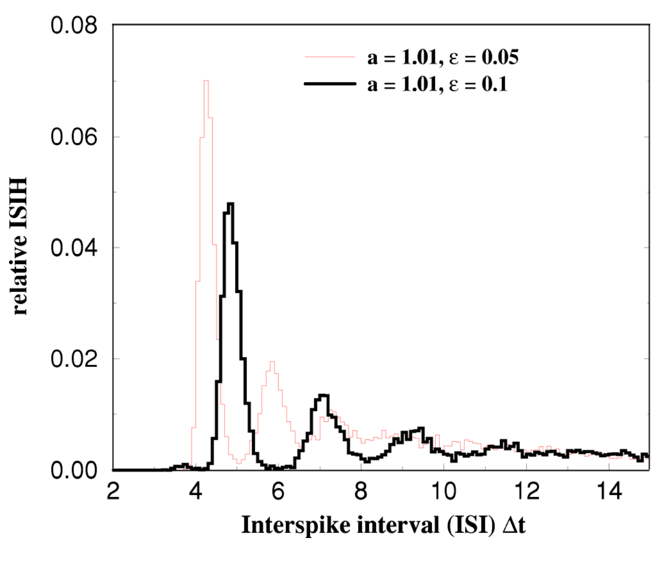

FIG. 3. ISIH in a noise driven excitable FHN model. The parameters are $a = 1.01$, $\varepsilon = 0.1$.

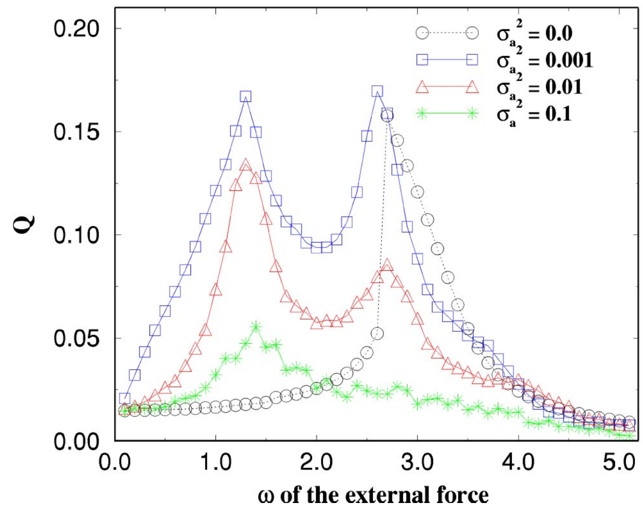

FIG. 4. Resonances for the periodically driven ($b = 0.03$) FHN system in the excitable regime ($a = 1.01$) under the influence of different noise intensities.

$$Q_{\cos} = \frac{\omega}{2n\pi}\int_0^{2\pi n/\omega} 2x(t)\cos(\omega t)\,dt,$$

$$Q = \sqrt{Q_{\sin}^2 + Q_{\cos}^2}.$$

First we look for the resonance frequencies of the system to find both internal frequencies (Canard frequency and frequency of the spiking behavior). Therefore we calculate the Q parameter versus the circle frequency of the driving force. We consider three cases: (a) $a = 1.01$, FHN in a monostable excitable regime; (b) $a = 1.0$, FHN at the bifurcation point; (c) $a = 0.998$, FHN in an oscillatory regime with small Canard oscillations around the unstable fix point and small amplitudes compared with the amplitude of a spike. The amplitude of the periodic driving force is chosen small enough so that the system needs noise to reach the threshold and to produce a spike. Figures 4–6 show the dependence of the Q

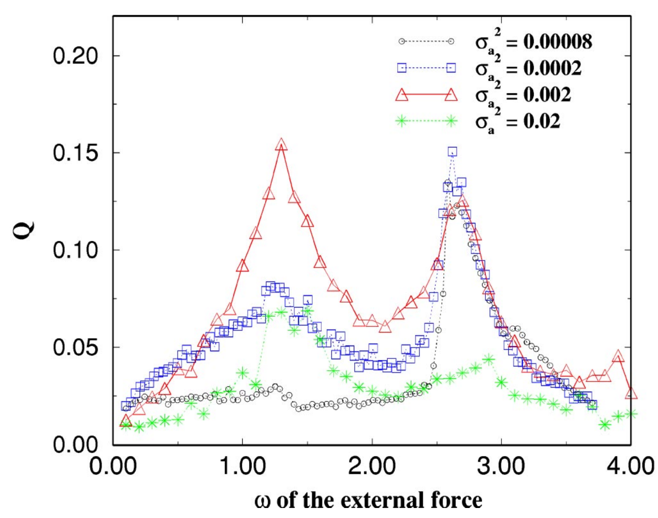

FIG. 5. Resonances for the periodically driven ($b = 0.02$) FHN system at the bifurcation point ($a = 1.0$) under the influence of different noise intensities.

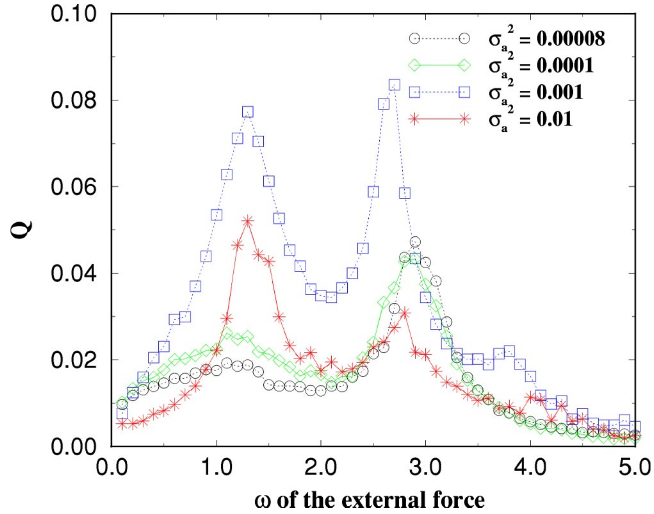

FIG. 6. Resonances for the periodically driven ($b=0.01$) FHN system in the oscillatory regime ($a=0.998$) under the influence of different noise intensities.

parameter on the input frequency for these three cases and various noise intensities σ_a^2. The Q parameter refers to the variable input frequency and measures the amplitude of the input frequency in the output signal.

The first peak in Figs. 4–6 at $\omega=1.3$ corresponds to a period length of $T=4.83$ and is caused by the firing of a spike. The second peak at about $\omega=2.6$–2.9 is caused by the Canard oscillations near the fix point x_f, y_f with a small amplitude compared with the big spike. In opposition to the resonance frequency of the spike, the position of the Canard resonance frequency Ω_C depends on the parameter a and the noise intensity σ_a^2. This can be also easily seen in the phase space in Figs. 1 and 2. The trace of the spikes is very stable and narrow, and so the time for one round-trip during a spike is independent of the parameter a and the noise, while the traces for the Canard oscillations fill a much wider area in the phase space. Hence we can observe a shifting of the Canard-resonance frequency by changing a and σ_a^2. It is important to note that a peak at the Canard frequency exists even for smaller noise intensities, when the peak at the spiking frequency is not yet pronounced. This explains the fact that adding the driving force at this Canard frequency can be successfully used in the improvement of a signal receiving, even if the information is carried by another low frequency.

Noteworthy, similar high-frequency resonance has been described recently in the Hodgkin-Huxley model [42] and it was proposed in the ‘‘resonate-and-fire’’ neuron model [43], but its background is the oscillatory convergence to the rest state instead of the Canard phenomenon. For a more stiff FHN oscillator, only the low-frequency peak in ISIH is observed, and its coherency is maximal if the period is equal to the time of cycle excursion as it has been shown in Ref. [28].

III. ENHANCEMENT OF STOCHASTIC RESONANCE

With the knowledge of the Canard-resonance frequency, we demonstrate that the response of the system to a given input frequency is improved. We force the FHN system with

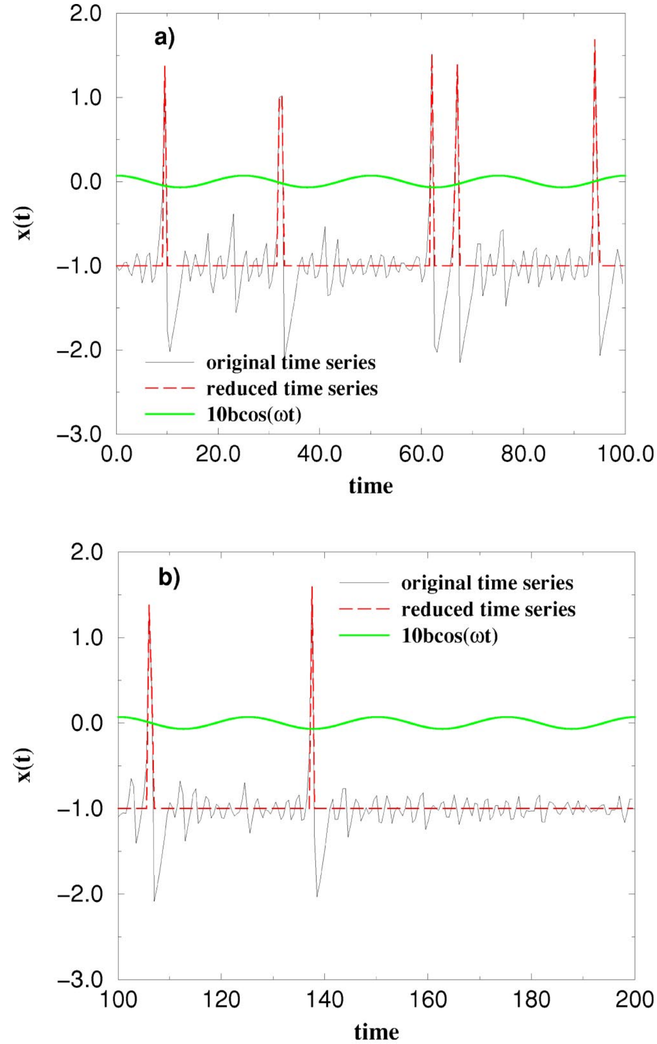

FIG. 7. Time series of the $x(t)$ variable for the excitable FHN system driven by additive noise and two periodic forces. The high-frequency input signal is in resonance with the Canard frequency (a) and out of resonance with the Canard frequency (b). For a better recognition of the signal processing with the low-frequency input signal, this periodic input signal is also plotted (with a ten times higher amplitude than in the model).

two different but fixed frequencies,

$$F_{ext}(t)=b\cos(\omega t)+C\cos(\Omega t).$$

The basic idea is that the information is stored in a low-frequency input signal with a circle frequency ω and an amplitude b. The additional high-frequency input signal $C\cos(\Omega t)$ and the noise helps to reach the threshold, so both are necessary to produce a spike. The amplitude of both periodic input signals are chosen small enough that they cannot produce a spike without noise. A similar situation was in the study of the vibrational resonance [38]. But the setup of the parameters in Ref. [38] did not allow use of the Canard resonance in the signal processing.

In Fig. 7, two typical time series of the x variable are plotted for the parameters $\varepsilon=0.1$, $a=1.01$, $\sigma_a^2=0.000\,375$,

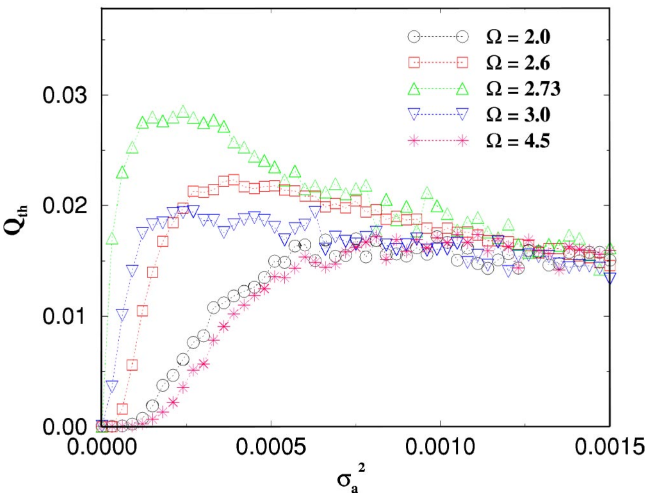

FIG. 8. Signal processing at the low-frequency (ω) input signal versus the noise intensity for various frequencies of the high-frequency input signals Ω for the FHN system in the excitable regime. Parameters: $a=1.01$, $b=0.007$, $C=0.025$, and $\omega=0.251$. The Canard-resonance frequency is $\Omega_C=2.73$, see Fig. 4.

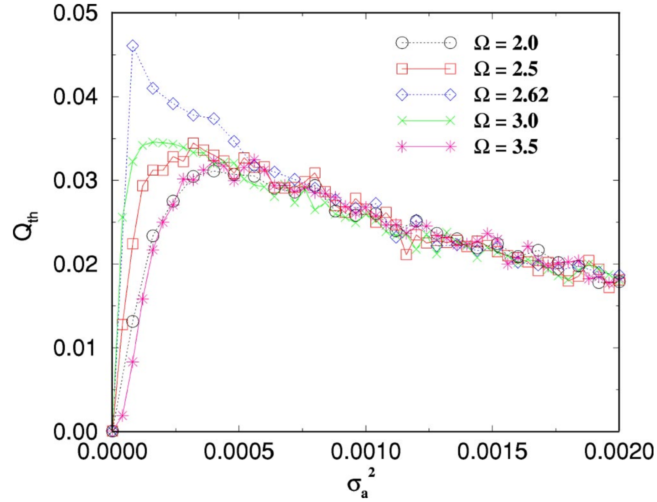

FIG. 9. Signal processing at the low-frequency (ω) input signal versus the noise intensity for various frequencies of the high-frequency input signals Ω for the FHN system at the bifurcation point. Parameters: $a=1.0$, $b=0.01$, $C=0.02$, and $\omega=0.251$. The Canard-resonance frequency is $\Omega_C=2.62$, see Fig. 5.

$C=0.025$, $b=0.007$, $\omega=0.251$, and $\Omega=2.73$ for Fig. 7(a) and $\Omega=2.0$, respectively, for Fig. 7(b). The difference between these two figures is the frequency Ω of the high-frequency input signal: the first one shows the case of resonant forcing with the Canard frequency ($\Omega=\Omega_C$) and the second one corresponds to the forcing out of the Canard frequency ($\Omega\neq\Omega_C$). As an important result, the amplitudes of the small oscillations around the fix point in the original time series $x(t)$ are different. Because of the resonance between the external high-frequency force and the noise-induced small amplitude oscillations in the Canard-resonant case, these small oscillations are enhanced by amplitude and the FHN in this regime can easier reach the threshold of the firing with the help of noise. As a result, we can observe the behavior that is more synchronized with the low-frequency input signal.

In natural systems with such a spiking behaviorlike neurons, only the spikes themselves are important for the information transport. As shown above, small Canard oscillations near the fix point are very important for the behavior of the FHN itself, but not for the information transport. To evaluate the information transport, we calculate again the response of the system, Q_{th}, but replace the original time series $x(t)$ by a reduced time series without oscillations around the fix point. In this way we consider only the spikes for the information transport. To distinguish between a spike and the subthreshold oscillations, we set the threshold of detection $x_{th}=0.0$. If $x(t)$ is smaller than x_{th}, we replace $x(t)$ by the value of the fix point x_f. For $x(t)\geqslant x_{th}$, we use the original value of $x(t)$. This replacement is used only for the calculation of the Q_{th} parameter and not for the simulation of the original time series with the Heun method. The filtered time series are also plotted in Fig. 7 by the dashed line. In Figs. 8–10 (excitable regime, at the bifurcation point, and oscillatory regime, respectively) the dependencies of the quality of the information transport (represented by the Q_{th} parameter at the low frequency ω) on the noise intensity σ_a^2 are depicted for different frequencies of the high-frequency driving force.

All three cases have in common that without noise ($\sigma_a^2=0$) we observe no information transport, because Q_{th} is zero. That means that the FHN system does not show a spiking behavior. These figures demonstrate the bell shaped form of Q_{th}, well-known SR effect [1], for all different high frequencies. In the range of lower noise, it can be clearly seen that for the HF part of the signal being in resonance with Canard frequency, the SR effect at the low frequency ω is significantly enhanced. In this region there is a significant difference in the Q_{th} parameter between the forcing at the

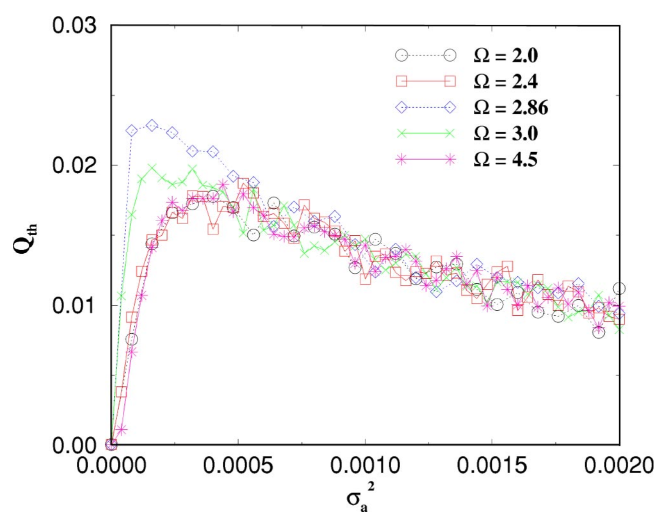

FIG. 10. Signal processing at the low-frequency (ω) input signal versus the noise intensity for various frequencies of the high-frequency input signals Ω for the FHN system in the oscillatory regime. Parameters: $a=0.998$, $b=0.005$, $C=0.01$, and $\omega=0.251$. The Canard-resonance frequency is $\Omega_C=2.86$, see Fig. 6.

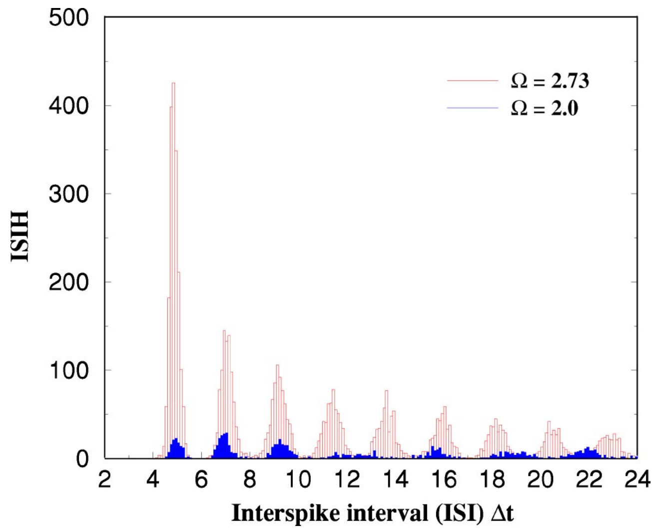

FIG. 11. ISI histogram by forcing of the excitable FHN system in ($\Omega = 2.73 = \Omega_C$) and out of the Canard resonance ($\Omega = 2.0 \neq \Omega_C$).

Canard-resonance frequency ($\Omega = \Omega_C$) and the forcing out of the Canard resonance ($\Omega \neq \Omega_C$). The difference in the Q_{th} parameter is caused only by a change of the frequency Ω of the HF signal because the amplitudes are the same within one figure. This effect can be understood as the coexistence of two resonances. The first resonance happens between the high frequency of a signal and the frequency of Canard oscillations. If these two frequencies are similar, this resonance amplifies the conventional SR for a signal with low frequency.

The demonstration of signal enhancement may be presented also in the form of interspike interval histograms. In Fig. 11 the ISIH is depicted for the same parameters ($\omega = 0.251$) which are used for both the time series in Figs. 7(a) and 7(b). Both ISIHs were calculated with the same length of 100 000 time units for the underlying time series in Canard resonance ($\Omega = 2.73 = \Omega_C$) and out of resonance ($\Omega = 2.0 \neq \Omega_C$). In the resonant case, much more spikes occur, and hence, the peaks of ISIH have higher values. The first maximum in the ISIH for both time series is between $\Delta t = 4.8$ and 4.9 and corresponds exactly to the resonance frequency of the spikes with period $T = 4.83$. The time of the first maximum is the minimal time between two adjacent spikes when one spike follows the other one without any waiting time, i.e., without any small Canard oscillation.

For the Canard-resonant case, we observe the expected multimodal structure with peaks located at multiples of the period length of the Canard oscillations or high-frequency force at $T = 2.3$ ($\Omega = 2.73$). This modulation is very regular. By forcing out of Canard resonance with $\Omega = 2.0$ or $T = 3.14$, the first three peaks are approximately at the same position as in the resonant case. Although we force out of the Canard frequency, one or two Canard periods can occur between two adjacent spikes. Except for these three peaks in the ISIH, the multimodal structure with the period of the Canard period is suppressed. For higher interspike intervals, a modulation with the period of $T \approx 3$ can be observed, which corresponds to the high-frequency input signal. In this case the Canard oscillation can succeed only for two periods and lose the competition with the high-frequency forcing after this time, and the waiting time will be dominated now by integer numbers of the high-frequency period.

IV. SUMMARY

In conclusion, we have considered a signal processing in the noisy system which possesses both oscillatory and excitable properties under the action of an additional HF signal. This system was represented by the FHN model with a stiffness between pure excitable and oscillatory regime. We have demonstrated the possibility to amplify the SR effect in such systems using the Canard oscillations. In this effect the HF signal that is in resonance with the frequency of Canard oscillations strongly improves signal processing of the low-frequency signal. The effect shows a frequency selectivity and disappears in the region out of resonance with the Canard frequency.

For supercritical Hopf bifurcation in FHN-like models, this phenomenon is relevant for biology if the stiffness of the system (a degree of excitability) is limited by the interval $\varepsilon \in [0.2 - 0.01]$ in order to get the observable periods of noise-induced Canard-like orbits. In this interval very small noise is necessary for a significant improvement of signal processing. It means, e.g., for neurons, the possibility of a new regulation of signal processing which, in addition to the choice of the value of the bifurcation parameter, can control the signal transmission under a small noisy environment.

We hope that these theoretical findings will stimulate experimental work to find new possibilities of signal receiving and propagation in systems, which demonstrate Canard-like oscillations, especially in nonlinear chemical systems [44] or in biophysical models [23,24]. Moreover, the dynamical systems, which have some specific regime between excitable and oscillatory states, are not limited by the FHN with Canard phenomenon. Recently, it has been shown that the modified Oregonator equations have three steady states and excitation occurs via resonance between damped HF oscillations around the stable fixed point and periodic perturbations with an appropriate tuning frequency [45]. A similar SR enhancement by HF signal may also be expected in this chemical system with low excitability.

ACKNOWLEDGMENTS

E.V. and J.K. acknowledge financial support from SFB 555 (Germany), E.U. from the International MP Research School on Biomimetic Systems, and A.Z. from the Microgravity Application Program/Biotechnogy of the European Space Agency.

[1] L. Gammaitoni, P. Hänggi, P. Jung, and F. Marchesoni, Rev. Mod. Phys. **70**, 223 (1998).
[2] R. Benzi, A. Sutera, and A. Vulpiani, J. Phys. A **14**, L453 (1981).
[3] P. Hänggi, Chem. Phys. **3**, 285 (2002).
[4] A. Zaikin, J. Kurths, and L. Schimansky-Geier, Phys. Rev. Lett. **85**, 227 (2000).
[5] K. Wiesenfeld *et al.*, Phys. Rev. Lett. **72**, 2125 (1994).
[6] R. Rozenfeld, J.A. Freund, A. Neiman, and L. Schimansky-Geier, Phys. Rev. E **64**, 051107 (2001).
[7] J. Douglas, L. Wilkens, and L. Pantazelou, Nature (London) **365**, 337 (1993).
[8] T. Mori and S. Kai, Phys. Rev. Lett. **88**, 218101 (2002).
[9] D. Russel, L. Wilkens, and F. Moss, Nature (London) **402**, 291 (1999).
[10] J. Lindner *et al.*, Phys. Rev. Lett. **75**, 3 (1995).
[11] S. Kádár, J. Wang, and K. Showalter, Nature (London) **391**, 770 (1998).
[12] A. Zaikin, J. García-Ojalvo, L. Schimansky-Geier, and J. Kurths, Phys. Rev. Lett. **88**, 010601 (2002).
[13] R. Reigada, A. Sarmiento, and K. Lindenberg, Phys. Rev. E **63**, 066113 (2001).
[14] J.F. Lindner, B.K. Meadows, W.L. Ditto, M.E. Inchiosa, and A.R. Bulsara, Phys. Rev. Lett. **75**, 3 (1995).
[15] J. Lindner *et al.*, Phys. Rev. E **63**, 041107 (2001).
[16] J. Lindner *et al.*, Phys. Rev. E **53**, 2081 (1996).
[17] F. Marchesoni, L. Gammaitoni, and A.R. Bulsara, Phys. Rev. Lett. **76**, 2609 (1996); J.M.G. Vilar and J.M. Rubí, *ibid.* **78**, 2886 (1997).
[18] H.S. Wio, Phys. Rev. E **54**, R3075 (1996); S. Bouzat and H.S. Wio, *ibid.* **59**, 5142 (1999).
[19] A. Neiman and W. Sung, Phys. Lett. A **223**, 341 (1996).
[20] A. Pikovksy and J. Kurths, Phys. Rev. Lett. **78**, 775 (1997).
[21] C. Heneghan *et al.*, Phys. Rev. E **54**, 2228 (1996).
[22] V.A. Makarov, V.I. Nekorkin, and M.G. Velarde, Phys. Rev. Lett. **86**, 3431 (2001).
[23] S. Baer and T. Erneux, SIAM (Soc. Ind. Appl. Math.) J. Appl. Math. **46**, 721 (1986).
[24] S. Schuster and M. Marhl, J. Biol. Systems **9**, 291 (2001).
[25] P. Glendinning, *Stability, Instability, and Chaos: An Introduction to the Theory of Nonlinear Differential Equations* (Cambridge University Press, Cambridge, 1994).
[26] F. Dumortier and R. Roussarie, Mem. Am. Math. Soc. **577**, 1 (1996).
[27] L. Alfonsi, L. Gammaitoni, S. Santucci, and A. Bulsara, Phys. Rev. E **62**, 299 (2000).
[28] S.R. Massanes and C.P. Vicente, Phys. Rev. E **59**, 4490 (1999).
[29] M. Inchiosa *et al.*, Phys. Rev. E **63**, 066114 (2001).
[30] J. Acebrón, W. Rappel, and A. Bulsara, Phys. Rev. E **67**, 016210 (2003).
[31] V. Mironov and V. Sokolov, Radiotekh. Elektron. (Moscow) **41**, 1501 (1996).
[32] J. Victor and M. Conte, Visual Neurosci. **17**, 959 (2000).
[33] D. Su, M. Chiu, and C. Chen, Precis. Eng. **18**, 161 (1996).
[34] A. Maksimov, Ultrasonics **35**, 79 (1997).
[35] C. Cho *et al.*, Pharmacol. Res. **19**, 1123 (2002).
[36] J. Karnes and H.W. Burton, Arch. Phys. Med. Rehabil. **83**, 1 (2002).
[37] O. Schlafer *et al.*, Ultrasonics **40**, 25 (2002).
[38] E. Ulnner, A. Zaikin, R. Bascones, J. García-Ojalvo, and J. Kurths, Phys. Lett. A **312**, 348 (2003).
[39] J. Das and H. Busse, Biophys. J. **60**, 369 (1991).
[40] S. Girard *et al.*, Biophys. J. **61**, 509 (1992).
[41] H. Mahara, T. Yamaguchi, and Y. Amagishi, Chem. Phys. Lett. **317**, 23 (2000).
[42] P. Parmananda, C.H. Mena, and G. Baier, Phys. Rev. E **66**, 047202 (2002).
[43] E.M. Izhikevich, Neural Networks **14**, 883 (2001).
[44] M. Brons and J. Sturis, Phys. Rev. E **64**, 026209 (2001).
[45] P. Parmananda, H. Mahara, T. Amemiya, and T. Yamaguchi, Phys. Rev. Lett. **87**, 238302 (2001).